

Electronic Supplementary Information

Self-crystallization of uniformly oriented zeolitic imidazolate framework films at air-water interface

Jingyi Su, Wufeng Wu, Zhanjun Li and Wanbin Li*

*School of Environment and Guangdong Key Laboratory of Environmental Pollution
and Health, Jinan University, Guangzhou 511443, P.R. China.*

Corresponding author E-mail: gandeylin@126.com

Experimental details:

Preparation of ZIF-8 films

Self-crystallization was carried out by simple water evaporation. Two precursor solutions with concentration of 200 mmol L⁻¹ were prepared by adding Zn(NO₃)₂•6H₂O and 2-methylimidazole (MeIM) into deionized water independently. For fabrication of ZIF-8 films, MeIM aqueous solution with volume of 25 mL and Zn(NO₃)₂•6H₂O aqueous solution with volume of 250 μL were mixed in a Petri dish with diameter of 5.0 cm. The concentration and volume of MeIM solution was constant, the volume of Zn(NO₃)₂•6H₂O solution was changed for obtaining mixed precursor solutions with different MeIM/Zn ratios of 400, 200, 100, 50 and 25. Then the Petri dish filled with mixed precursor solution was heated at 50 °C. After evaporation for 8 h, a thin film was formed and floated on water surface.

Characterizations

The porosity of the film was characterized by using a physisorption analyzer (Autosorb iQ Station 1, Quantachrome Co.). The sample was prepared by stirring the formed ZIF-8 film and then filtration. The sample was treated in vacuum at 150 °C for 12 h before measurement. Nitrogen adsorption-desorption isotherms were recorded at 77.35 K held using liquid nitrogen bath. The specific surface area was calculated by using Multi-Point Brunauer-Emmett-Teller (BET) method with P/P₀ range from 0.003-0.05. Pore width was achieved by Density Functional Theory method. The XRD patterns were acquired with an XRD diffractometer (D2 Phaser,

Bruker CO) at 30kV and 10mA. The chemical structure was obtained by Fourier transform infrared spectrometer (FTIR, IRTracer-100, Shimadzu CO.). X-ray photoelectron spectroscopy (XPS) experiments was carried out by using a RBD upgraded PHI-5000C ESCA system (Perkin Elmer) with an incident radiation of monochromatic Mg K α X-rays ($h\nu=1253.6$ eV) at 250 W. The spectra of all the elements were collected by using RBD 147 interface (RBD Enterprises, USA). The morphology of the obtained membranes was determined by a field-emission scanning electron microscope (SEM, Ultra-55, Zeiss Co.) at 5 kV. Transmission electron microscopy (TEM) images of the ZIF-8 films and plates were captured by using the JEM-2100 (JEOL Co.). The accelerating voltage was 200 kV. For preparation of samples, The ZIF-8 films and plates were loaded on the ultrathin carbon films with copper nets and subjected to dry at atmosphere. The attached X-ray energy dispersion spectroscope (EDS) was applied to investigate the element distribution of the prepared films and plates. An atomic force microscope (AFM, Bioscope Catylyst Nanoscope-V, Bruker, USA) was employed to test the surface morphology of the prepared films. The samples were loaded on the mica plates for measurement. NanoScope Analysis software (Version 1.4) was applied to calculated the root mean square roughness (R_q) and arithmetic average roughness (R_a).

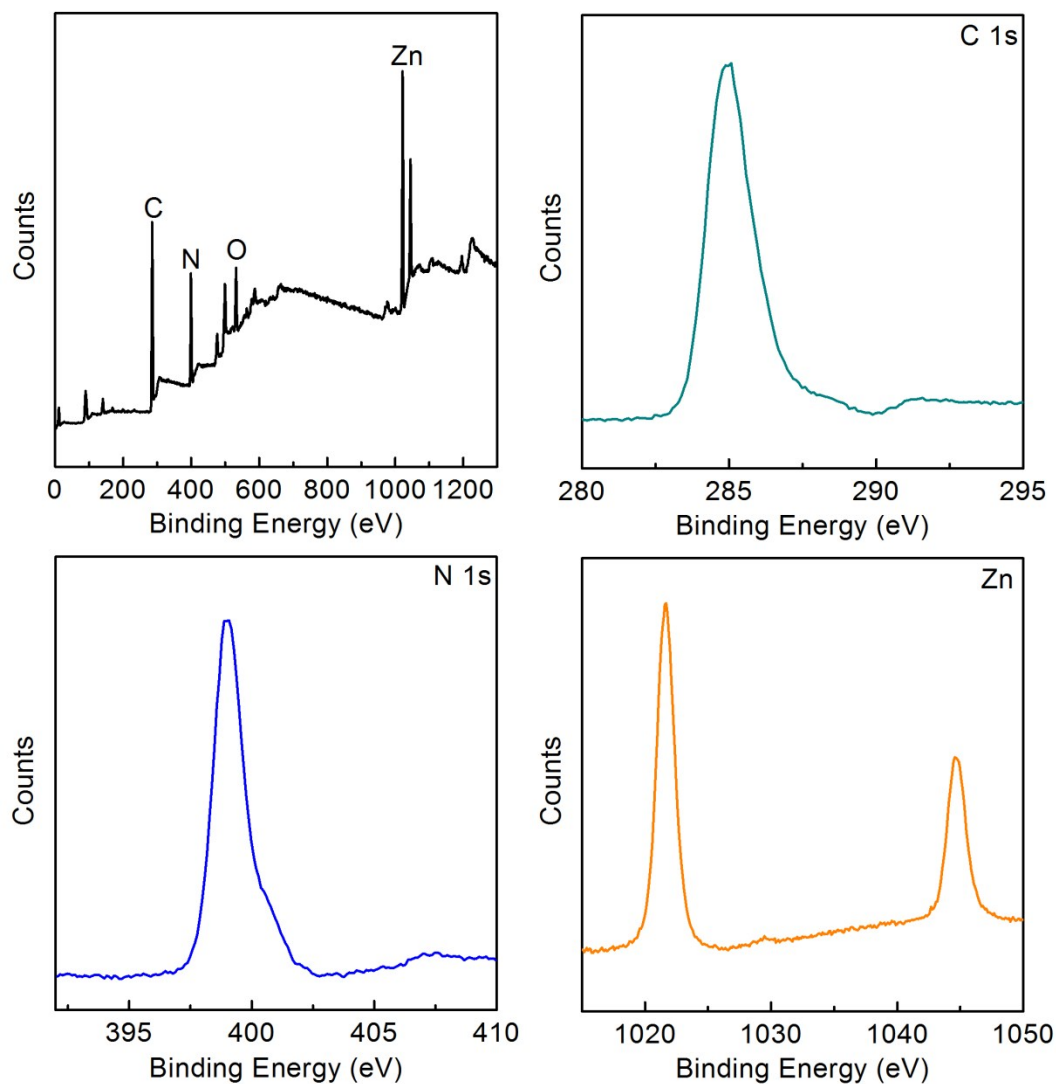


Fig. S1 XPS survey spectrum, and high-resolution C 1s, O 1s and Zn XPS spectra of the ZIF-8 film prepared with MeIM concentration of 200 mmol L⁻¹ and MeIM/Zn ratio of 100. XPS spectrum shows the peaks for carbon, nitrogen, oxygen and zinc. The atomic contents of carbon, nitrogen, oxygen and zinc are 61.26%, 22.69%, 8.40% and 7.65%, respectively. The existence of oxygen is interpreted by the interaction between the zinc nodes and hydroxyls.

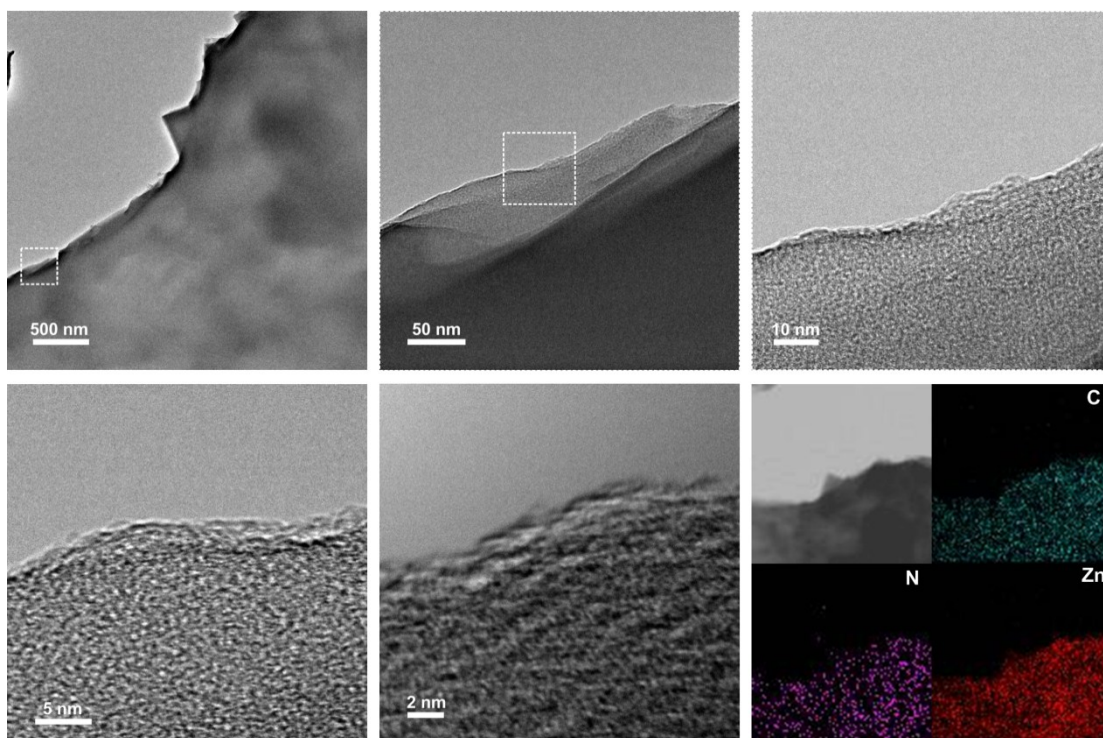


Fig. S2 TEM images with various magnifications and EDS mapping images of the ZIF-8 film prepared with MeIM concentration of 200 mmol L^{-1} and MeIM/Zn ratio of 100. Since ZIF-8 is sensitive to the high-energy electron beam, it is difficult to capture the image with clear lattice structure by the applied high-resolution transmission electron microscope with acceleration voltage of 200 kV. EDS mapping images of the ZIF-8 film indicate the homogeneous distributions of carbon, nitrogen and zinc.

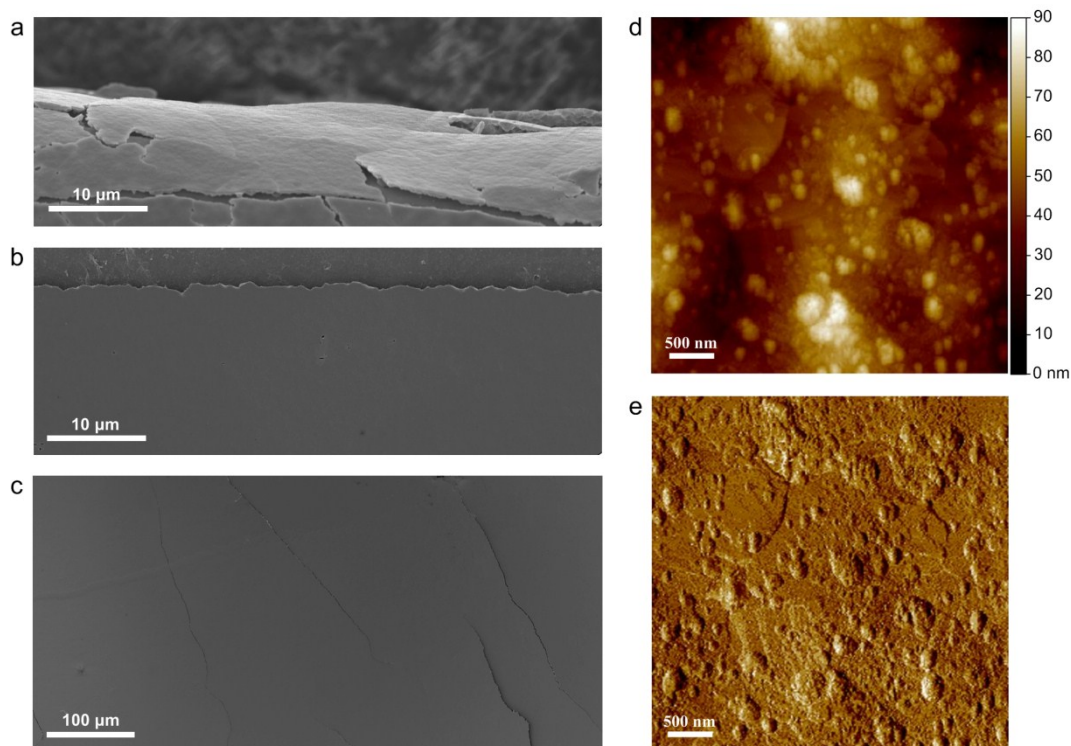


Fig. S3 (a) Cross-sectional view SEM image with low magnification of the ZIF-8 film. (b,c) SEM images with low magnification of the top air-contacted side of the ZIF-8 film. (d) Height and (e) inphase AFM images of the ZIF-8 film. The ZIF-8 film prepared with MeIM concentration of 200 mmol L^{-1} and MeIM/Zn ratio of 100 was held by the mica plate. These images indicate that the formed ZIF-8 film is uniform at large scale. AFM images reveal that the air-contacted side has small roughness with root mean square roughness and arithmetic average roughness of only 12.0 and 9.2 nm, respectively.

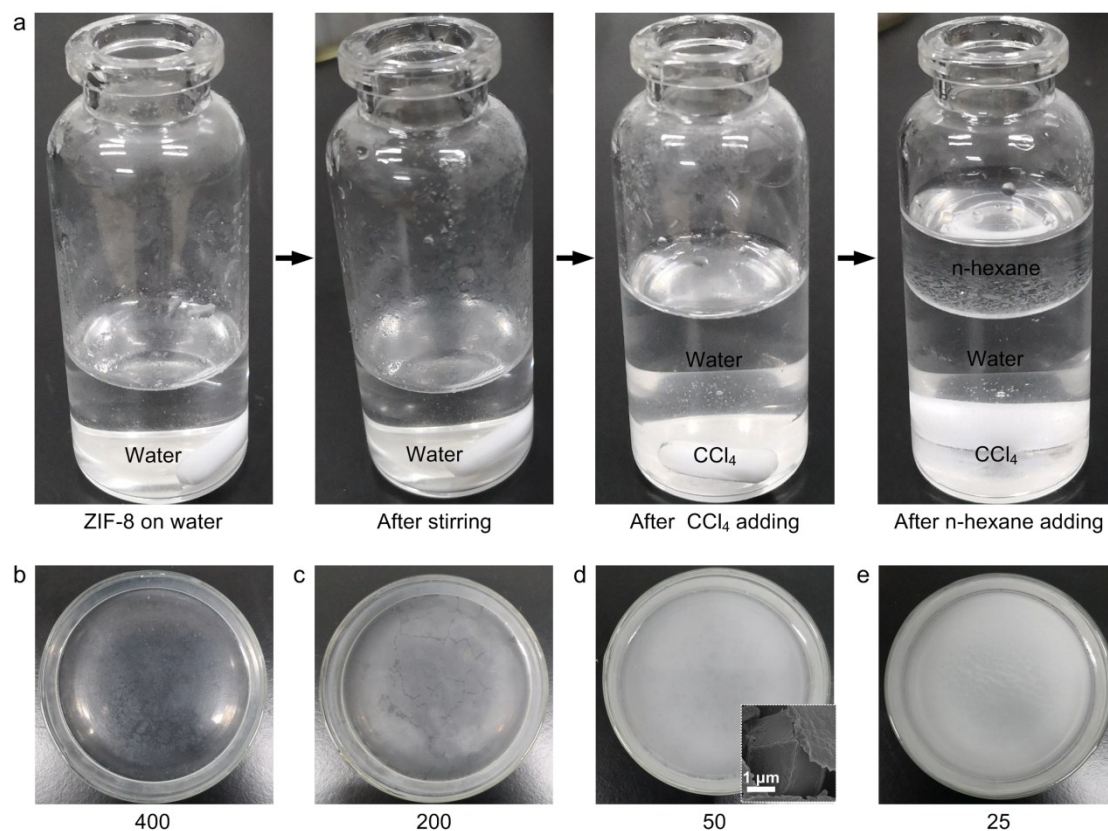


Fig. S4 (a) Photographs of the ZIF-8 fragments at interfaces of air-water, water-CCl₄ and n-hexane-water. Photographs of the ZIF-8 films prepared with ratios of (b) 400, (c) 200, (d) 50 and (e) 25. After adding non-polar CCl₄ and n-hexane, the fragments migrated to the immiscible interfaces between non-polar solvents and water, illustrating the different hydrophilic properties of two sides of the formed ZIF-8 film. Since the concentration exceeds the critical crystallization point, it is obvious that the crystals in bulk solution occur during the fabrication of the ZIF-8 films with MeIM/Zn ratios of 50 and 25. The inset in d indicates that the bulk crystals has rhombic dodecahedra structure with exposed {011} facet.

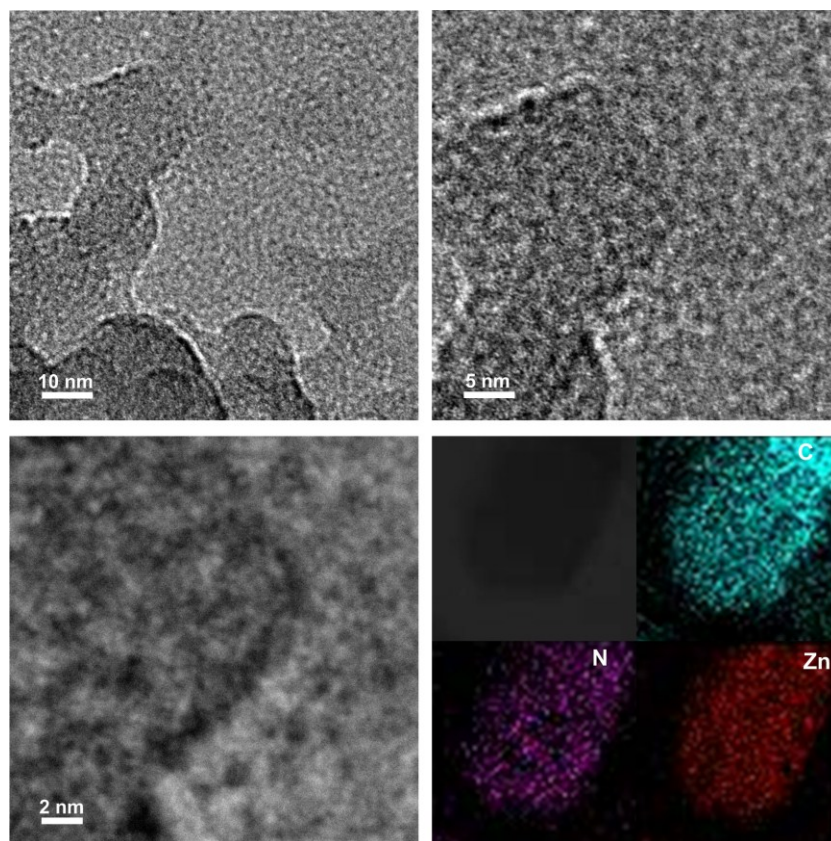


Fig. S5 TEM images with various magnifications and EDS mapping images of the ZIF-8 plates fabricated with MeIM concentration of 200 mmol L⁻¹, MeIM/Zn ratio of 100 and duration time of 4 h. The white spots and black dots suggest the porous structure of the ZIF-8 plates. EDS mapping images of the ZIF-8 plates indicate the homogeneous distributions of carbon, nitrogen and zinc.

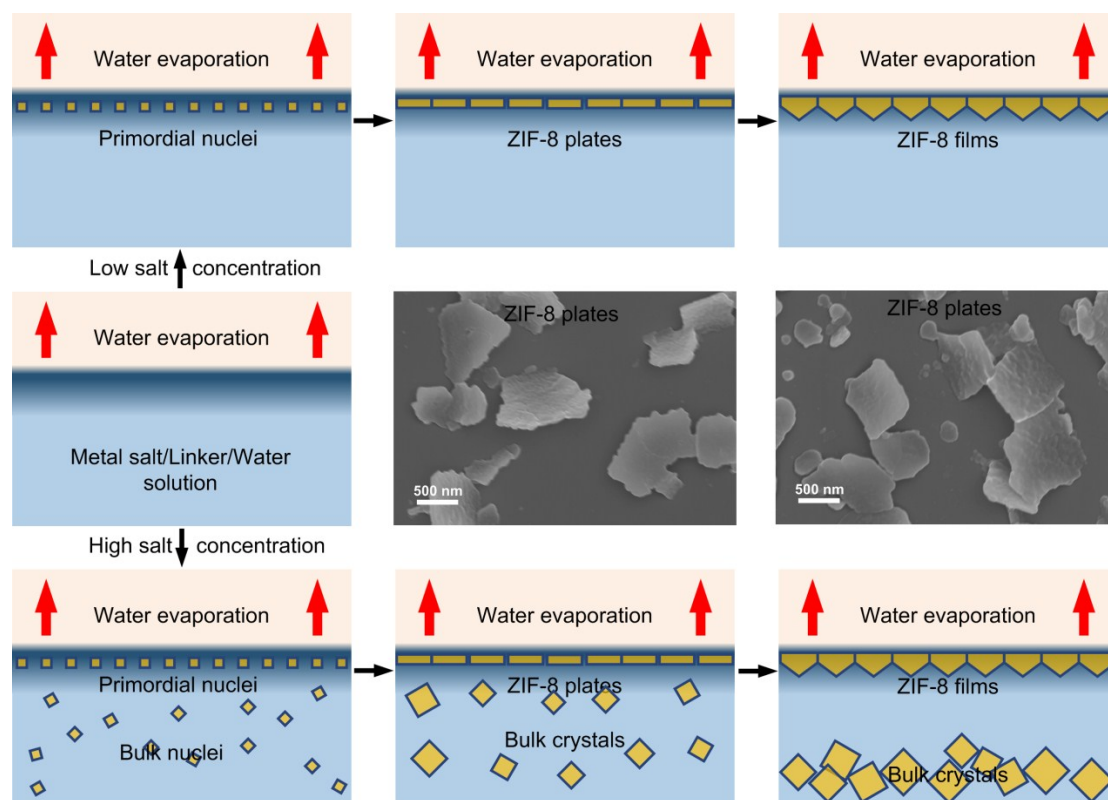


Fig. S6 Growth processes of ZIF-8 films. Top schematics present the growth process of the ZIF-8 films with larger ratios of 400, 200 and 100. For these ratios, there no homogeneous crystal is formed. Bottom schematics show the growth process of the ZIF-8 films with smaller ratios of 50 and 25. For these ratios, homogeneous nucleation leads to the formation of bulk ZIF-8 crystals. The evaporation causes the formation of primordial nuclei at interface. SEM images display the ZIF-8 plates prepared with duration time of 4 h. The growth process at interface has the growth order from primordial nuclei to plates and then films.

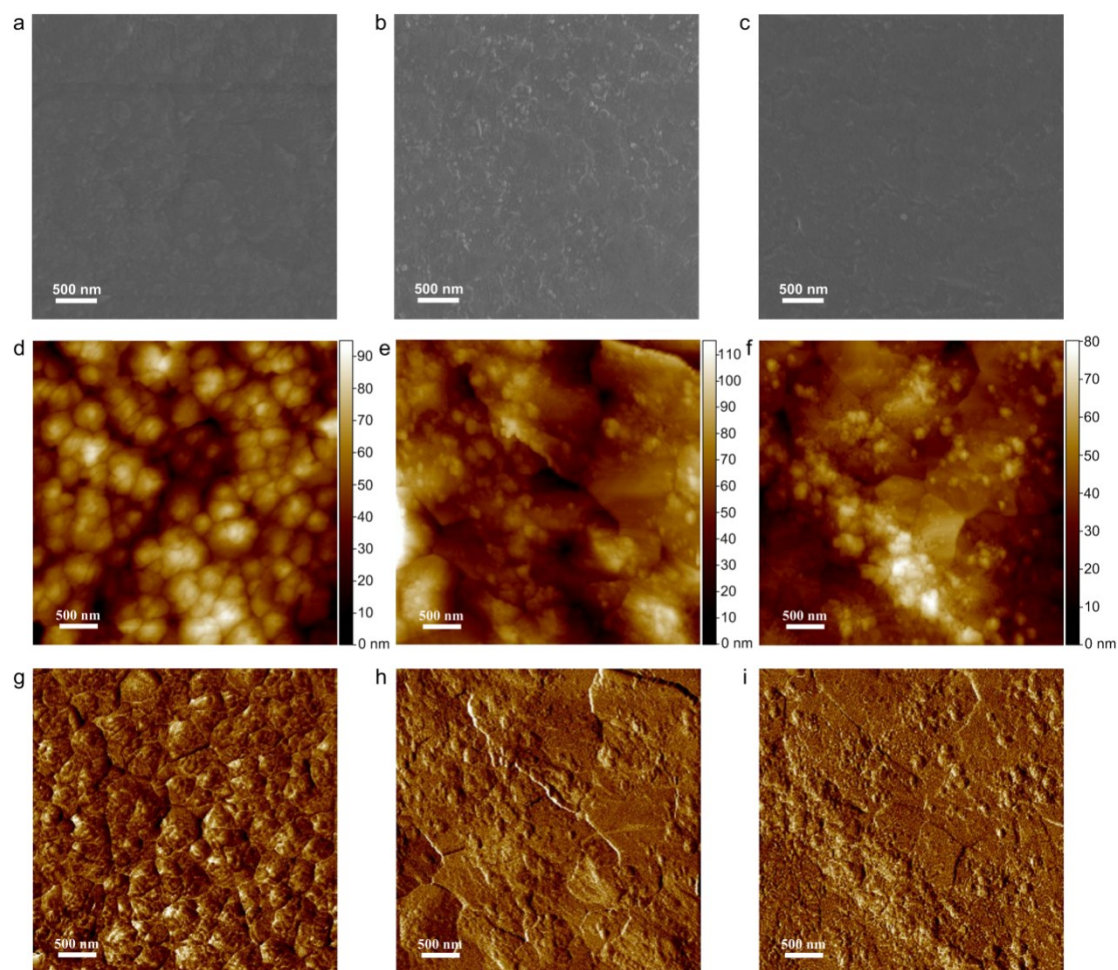


Fig. S7 SEM images of the air-contacted side of the ZIF-8 films with MeIM/Zn ratios of (a) 400, (b) 200 and (c) 50. (d-f) Height and (g-i) inphase AFM images of the air-contacted side of the ZIF-8 films synthesized with ratios of (d,g) 400, (e,h) 200 and (f,i) 50. All samples were fabricated with MeIM concentration of 200 mmol L⁻¹. The values of R_q/R_a for the films prepared with ratios of 400, 200 and 50 are 13.8/10.8, 15.1/11.9 and 11.2/8.9 nm, respectively.

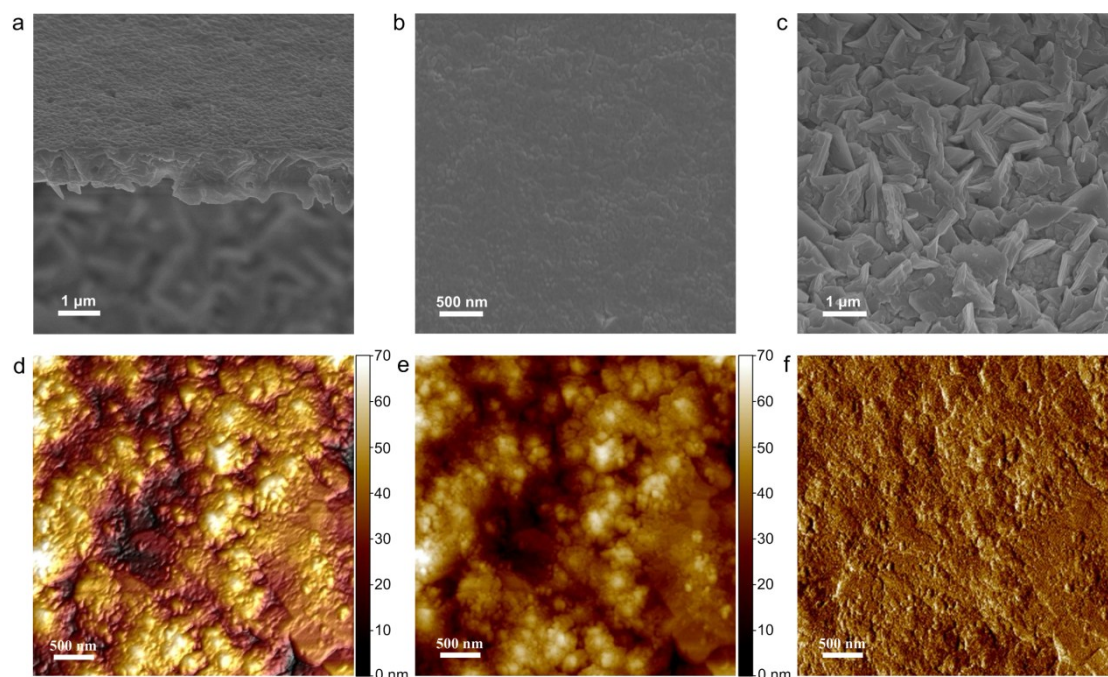


Fig. S8 (a) Cross-sectional view, (b) air-contacted side and (c) water-contacted side SEM images of the ZIF-8 film prepared with MeIM concentration of 200 mmol L⁻¹ and MeIM/Zn ratio of 25. (d) 3-D height, (e) height and (f) inphase AFM images of the ZIF-8 film. The ZIF-8 film displays Janus structures with smooth air-contacted side and rough water-contacted side. Unlike the films with other MeIM/Zn ratios, which exhibit hemi rhombic dodecahedra structures, the film with MeIM/Zn ratio of 25 shows an anomalous water-contacted structure. This result is interpreted by the rapid growth and homogeneous crystallization of ZIF-8 under high metal salt concentration. The values of R_q and R_a for the films prepared ratio of 25 were 9.8 and 7.8 nm, respectively.

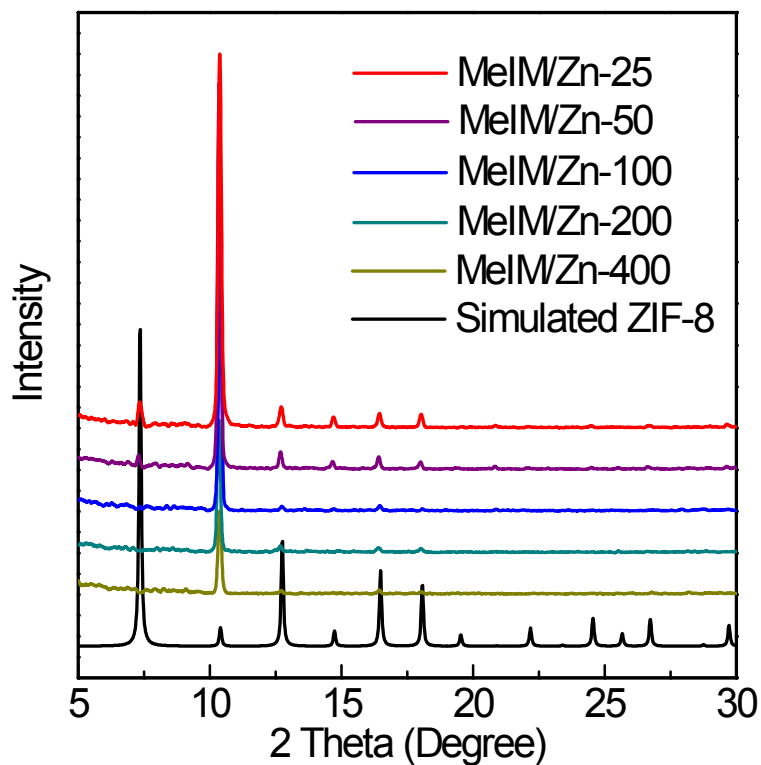


Fig. S9 XRD patterns of ZIF-8 films with various precursor ratios. With the decrease of MeIM/Zn ratio and the increase of metal salt concentration, the intensity of the characteristic peaks for {011}, {112}, {013} and {222} facets is stronger. The simulated XRD pattern is presented for comparison. All films were prepared with MeIM concentration of 200 mmol L⁻¹. The amorphous anodic aluminum oxide substrate was employed for holding the ZIF-8 films.

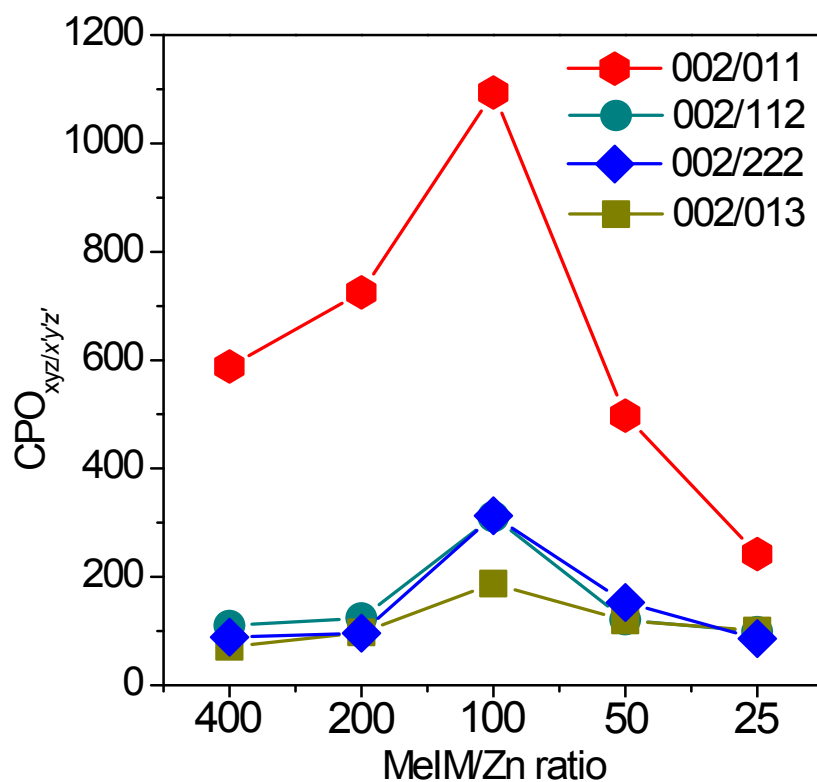


Fig. S10 CPO_{xyz/x'y'z'} of ZIF-8 films with various precursor ratios. With the decrease of MeIM/Zn ratio and the increase of metal salt concentration, the values of CPO_{002/011}, CPO_{002/112}, CPO_{002/222} and CPO_{002/013} first increase and then decrease. The corresponding values are presented in Table S1.

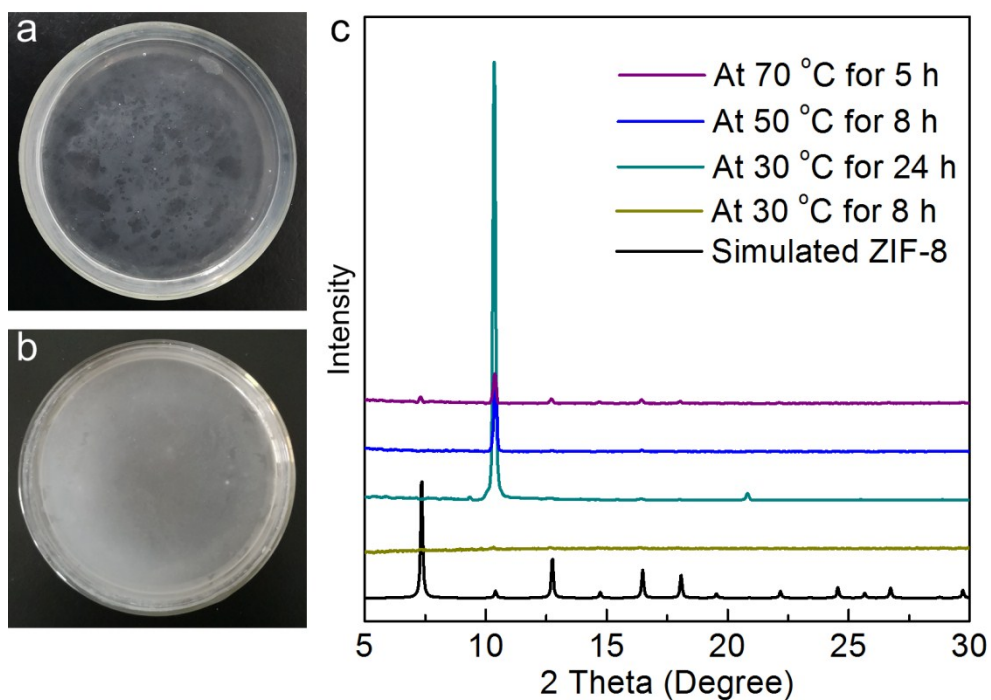


Fig. S11 Photographs of the ZIF-8 films prepared at (a) 30°C for 8 h and (b) 70 °C for 5 h. (c) XRD patterns of the ZIF-8 films prepared at 30, 50 and 70 °C. XRD pattern of the simulated ZIF-8 is presented for comparison. The ZIF-8 films were prepared with MeIM concentration of 200 mmol L⁻¹ and MeIM/Zn ratio of 100. It should be noted that the 8-h treatment at 70 °C causes the water to be evaporated completely. The out-of-plane orientation of the film prepared at 30 °C for 24 h is even better than that of the film prepared at 50 °C for 8 h.

Table S1. CPO values of the ZIF-8 films with various ratios. $CPO_{xyz/x'y'z'}$ indicates the relationship of the dominant $\{xyz\}$ facet to corresponding $\{x'y'z'\}$ facet. The values of CPO increase firstly and then decrease as MeIM/Zn ratio reduction. $CPO_{xyz/x'y'z'}$ is calculated by the intensity of corresponding peaks from experimental and simulated XRD patterns. For example, $CPO_{002/011}$ was calculated by $(I_{002}^e/I_{011}^e)/(I_{002}^s/I_{011}^s)$. Where the I_{002}^e and I_{011}^e are the intensities of peaks for $\{002\}$ and $\{011\}$ facets from experimental XRD patterns, the I_{002}^s and I_{011}^s are the intensities of peaks for $\{002\}$ and $\{011\}$ facets from simulated XRD patterns.

MeIM/Zn	$CPO_{002/01}$	$CPO_{002/11}$	$CPO_{002/013}$	$CPO_{002/222}$
	1	2		
400	588.4	109.8	70.6	88.6
200	725.4	124.0	97.4	96.0
100	1094	311.0	187.7	313.1
50	497.8	120.8	119.2	152.9
25	242.0	98.4	100.6	86.3